

# Defective peroxisomal proliferators activated receptor gamma activity due to dominant-negative mutation synergizes with hypertension to accelerate cardiac fibrosis in mice

Adrienn Kis<sup>1†</sup>, Colin Murdoch<sup>2†</sup>, Min Zhang<sup>2</sup>, Anjana Siva<sup>2</sup>, Sergio Rodriguez-Cuenca<sup>1</sup>, Stefania Carobbio<sup>1</sup>, Agnes Lukasik<sup>1</sup>, Margaret Blount<sup>1</sup>, Steve O’Rahilly<sup>1</sup>, Sarah L. Gray<sup>3</sup>, Ajay M. Shah<sup>2\*</sup>, and Antonio Vidal-Puig<sup>1\*</sup>

<sup>1</sup>Metabolic Research Laboratories, Level 4, Institute of Metabolic Sciences, Box 289, Addenbrooke’s Hospital, Cambridge CB2 0QQ, UK; <sup>2</sup>Cardiovascular Division, King’s College London British Heart Foundation Centre of Research Excellence, 125 Coldharbour Lane, London SE5 9NU, UK; and <sup>3</sup>Northern Medical Program, University of Northern British Columbia, 3333 University Way, Prince George BC, Prince George BC V2N 479, Canada

Received 9 September 2008; revised 12 February 2009; accepted 26 February 2009; online publish-ahead-of-print 24 April 2009

## Aims

Humans with inactivating mutations in peroxisomal proliferators activated receptor gamma (PPAR $\gamma$ ) typically develop a complex metabolic syndrome characterized by insulin resistance, diabetes, lipodystrophy, hypertension, and dyslipidaemia which is likely to increase their cardiovascular risk. Despite evidence that the activation of PPAR $\gamma$  may prevent cardiac fibrosis and hypertrophy, recent evidence has suggested that pharmacological activation of PPAR $\gamma$  causes increased cardiovascular mortality. In this study, we investigated the effects of defective PPAR $\gamma$  function on the development of cardiac fibrosis and hypertrophy in a murine model carrying a human dominant-negative mutation in PPAR $\gamma$ .

## Methods and results

Mice with a dominant-negative point mutation in PPAR $\gamma$  (P465L) and their wild-type (WT) littermates were treated with either subcutaneous angiotensin II (AngII) infusion or saline for 2 weeks. Heterozygous P465L and WT mice developed a similar increase in systolic blood pressure, but the mutant mice developed significantly more severe cardiac fibrosis to AngII that correlated with increased expression of profibrotic genes. Both groups similarly increased the heart weight to body weight ratio compared with saline-treated controls. There were no differences in fibrosis between saline-treated WT and P465L mice.

## Conclusion

These results show synergistic pathogenic effects between the presence of defective PPAR $\gamma$  and AngII-induced hypertension and suggest that patients with PPAR $\gamma$  mutation and hypertension may need more aggressive therapeutic measures to reduce the risk of accelerated cardiac fibrosis.

## Keywords

Hypertension • Left ventricular hypertrophy • Interstitial fibrosis • Dominant-negative PPAR $\gamma$  • Lipodystrophy

## Introduction

Peroxisomal proliferators activated receptor gamma (PPAR $\gamma$ ) is an important transcription factor that controls metabolic aspects such

as adipogenesis and insulin sensitivity. Its relevance in controlling energy homeostasis is illustrated by the fact that humans with mutations in PPAR $\gamma$  typically develop severe metabolic complications characterized by insulin resistance, diabetes, lipodystrophy,

<sup>†</sup> The first two authors contributed equally to the study.

\* Corresponding author. Tel: +44 1223 762790, Email: ajv22@medschl.cam.ac.uk (A.V.-P.) and Tel: +44 20 7848 5189, Fax: +44 20 7848 5193, Email: ajay.shah@kcl.ac.uk (A.M.S.)

Published on behalf of the European Society of Cardiology. All rights reserved. © The Author 2009. For permissions please email: journals.permissions@oxfordjournals.org.

The online version of this article has been published under an open access model. Users are entitled to use, reproduce, disseminate, or display the open access version of this article for non-commercial purposes provided that the original authorship is properly and fully attributed; the Journal, Learned Society and Oxford University Press are attributed as the original place of publication with correct citation details given; if an article is subsequently reproduced or disseminated not in its entirety but only in part or as a derivative work this must be clearly indicated. For commercial re-use, please contact journals.permissions@oxfordjournals.org

hypertension, and dyslipidaemia; a cluster of metabolic alterations known to increase cardiovascular risk.<sup>1</sup> There is evidence that the activation of PPAR $\gamma$  using thiazolidinediones improves the metabolic control of diabetic patients<sup>2</sup> and that agonism of the PPAR $\gamma$  receptor may provide added beneficial cardiovascular effects by preventing cardiac fibrosis and hypertrophy.<sup>3</sup> However, the potential cardiovascular beneficial effects of PPAR $\gamma$  agonism have recently been questioned based on the evidence that rosiglitazone treatment to diabetic individuals may cause an increase in cardiovascular mortality of an unclear mechanism.<sup>4,5</sup> This observation has important clinical implications not only for its impact of treatment with PPAR $\gamma$  agonists on the therapeutic management and mental health of the diabetic population, but also for a relatively small subset of patients with mutations in PPAR $\gamma$  affected by a severe metabolic phenotype. In this study, we use a genetically humanized mouse model harbouring a well-characterized human PPAR $\gamma$  dominant-negative mutation to determine the effects of defective PPAR $\gamma$  function on cardiac contraction, fibrotic and hypertrophic responses under basal conditions and in the context of angiotensin II (AngII)-induced hypertension.

Hypertensive heart disease and cardiac hypertrophy, often associated with insulin resistance, are leading causes of high morbidity and mortality due to the predisposition to the development of congestive cardiac failure and sudden death. During this process, remodelling of the heart takes place contributing to persistent contractile dysfunction<sup>6</sup> and in numerous cases to arrhythmia.<sup>7</sup> Although the precise mechanisms underlying cardiac remodelling remain under intensive investigation, the involvement of increased activity of the renin–angiotensin–aldosterone system is well recognised<sup>7</sup>—as indicated by experimental models of aldosterone or AngII-induced hypertension where a similar process of remodelling occurs.<sup>8</sup>

Despite its low abundance in the heart, a direct role of PPAR $\gamma$  in cardiac hypertrophy has been hypothesised previously. It has been suggested that maximal transcriptional activity of PPAR $\gamma$  may delay the development of this pathological condition as indicated by the fact that ligands of PPAR $\gamma$  (troglitazone, pioglitazone, 15 $\delta$ -PGJ<sub>2</sub>) are able to prevent AngII-induced hypertrophy of neonatal rat cardiomyocytes.<sup>9,10</sup> Conversely, pioglitazone only marginally attenuated the hypertrophic response during pressure overload in mice that were heterozygous for deficient PPAR $\gamma$  compared with their wild-type (WT) littermates.<sup>10</sup>

The role of PPAR $\gamma$  in cardiac fibrosis is not fully understood. Remodelling and fibrosis take place following myocardial ischaemia, with an increase in myocardial collagen deposition, and predisposes to the development of heart failure. There is data suggesting that pioglitazone in mice<sup>11</sup> and rosiglitazone in rats<sup>12</sup> may reduce post-ischaemic myocardial collagen content and the degree of fibrosis, when these PPAR $\gamma$  ligands were administered after ischaemia. Similarly, in cardiac hypertrophy induced by transverse aortic constriction in rats, the PPAR $\gamma$  ligand rosiglitazone reduced collagen deposition and cardiac fibrosis.<sup>13</sup>

In this study, we use a genetic approach to investigate the effects of a human equivalent mutation of PPAR $\gamma$  (P465L dominant-negative point mutation) on the hypertrophic and fibrotic responses to chronic AngII-induced hypertension.

## Methods

### Animals

Peroxisomal proliferators activated receptor gamma (P465L) mice were generated as described before.<sup>14</sup> The age of 14-week-old male WT and heterozygous (P465L) littermate mice carrying 'knock-in' mutation were used in this study. Homozygous allelic combination of this mutation causes embryonic lethality. Experiments were performed in accordance with the Guidance on the Operation of Animals (Scientific Procedure) Acts, 1986 (UK).

### Experimental protocol

Osmotic minipumps (Alzet Model 1002, Charles River UK Ltd, Margate, UK) releasing either AngII at a dose of 1.1 mg kg<sup>-1</sup> day<sup>-1</sup> for 14 days or saline were implanted subcutaneously under isoflurane anaesthesia (2% isoflurane+98% O<sub>2</sub>). Wild-type and P465L heterozygous animals were randomized into the following experimental groups: WT mice treated with saline (WT/Sal; total  $n = 11$ ), P465L heterozygous mice treated with saline (P465L/Sal; total  $n = 11$ ), WT mice treated with AngII (WT/AngII; total  $n = 21$ ), and P465L heterozygous mice treated with AngII (P465L/AngII; total  $n = 22$ ).

### Non-invasive blood pressure measurement

Systolic blood pressure was measured by tail cuff plethysmography (Kent Scientific, Kings Hill, UK) in conscious mice at a temperature of 26°C following a 3 days training session. Blood pressure was measured on day 0, 7, and 14.

### Cardiac functional assessment by echocardiography

Under isoflurane anaesthesia (1.5% isoflurane and 98.5% O<sub>2</sub>), animals were placed on a heating pad in a supine position ( $n \geq 6$  per group). Echocardiographic images were acquired using a Sonos 5500 ultrasound system with a 15 MHz linear probe (Philips, Bothell, Washington) as described previously.<sup>15</sup> Two-dimensional LV short-axis views were acquired at the papillary muscle level and M-mode recordings were made. Depth settings were adjusted to maximize frame rate (220–260 Hz) and optimize temporal resolution. The interventricular septal thickness in diastole and the left ventricular end-diastolic and end-systolic dimensions were measured using three consecutive cycles. Fractional shortening and heart rate were calculated. Echocardiography was performed at day 7 and 14.

### Tissue collection and histology

At the end of the 14 days treatment, animals were sacrificed and body weight, atrial, right ventricular and left ventricular weights were measured. Upon tissue harvest, one third of the left ventricle (base) was separated for histological analysis approximately at the level of the papillary muscles and the remaining tissue was frozen in liquid nitrogen. Interstitial fibrosis was determined on formalin fixed, paraffin-embedded 4  $\mu$ m thick whole left ventricular sections using picrosirius red staining ( $n = 6–10$  per group). The density of collagen (pixel number) in heart sections was measured under polarized light based on its birefringence property at  $\times 200$  magnification in areas selected randomly, and was expressed as a percentage in relation to the total pixel number.

### Real-time polymerase chain reaction

Approximately 70–80 mg of frozen left ventricular tissue was used for total RNA extraction using Stat-60 (Tel-Test Co, Friendswood, USA).

**Table 1** Primer sequences used for reverse transcriptase-polymerase chain reaction

Protein	Gene	Allocation	Sequences 5'→3'
Procollagen I	<i>Col 1a1</i>	NM_007742	F: CCTCAGGGTATTGCTGGACAAC R: TTGATCCAGAAGGACCTTGTTTG
Procollagen III	<i>Col 3a1</i>	NM_009930	F: AGGAGCCAGTGCCATAATG R: TGACCATCTGATCCAGGGTTTC
Osteopontin	<i>Spp1</i>	NM_009263	F: GATTTGCTTTTGCTGTTTGG R: TGAGCTGCCAGAATCAGTCACT
Thrombospondin1	<i>Thbs1</i>	NM_011580	F: GGGGCAGGAAGACTATGACA R: CTCCCCGTTTTGTCTGTGT
PPAR $\gamma$ 1	<i>Pparg</i>	NM_011146	F: TTTAAAAACAAGACTACCCTTTACTGAAATT R: AGAGGTCCACAGAGCTGATTC Probe: GAGAGATGCCATTCTGGCCAC
Adiponectin	<i>AdipoQ</i>	NM_009605	F: CAGTGGATCTGACGACACCAA R: TGGGCAGGATTAAGAGGAACA Probe: AGGGCTCAGGATGCTACTGTTGCAAGC
Atrial natriuretic peptide precursor	<i>Nppa</i>	NM_008725	F: TGCGGTGTCCAACACAGATC R: CCTTCATCTTCTACCGGCATCTT
Skeletal muscle Alpha-actin	<i>Acta1</i>	NM_009606	F: CACCCAGGGCCAGAGTCA R: AGAGCGGTGGTCTCGTCTTC
Nox2	<i>Cybb</i>	NM_007807	F: TGTGTCGAAATCTGCCTCTCCTTT R: TTCCTGTCCAGTTGTCTTCGAA
Nox4	<i>Nox4</i>	NM_015760	F: CCGGACAGTCTGGCTTATC R: TGCTTTTTATCCAACAATCTTCTTGT
p22phox	<i>Cyba</i>	NM_007806	F: TGGACGTTTCACACACAGTGGT R: TGGACCCCTTTTTCTCTTT
p67phox	<i>Ncf2</i>	NM_010877	F: CTTTCATGTTGGTTGCCAATG R: AAGCTGTTTGCCTGTGAGGT

Single strand cDNA was synthesized by Im-Prom II reverse transcriptase according to the manufacturer's instructions (Promega, Southampton, UK) from 1000 ng RNA. Cardiac hypertrophy markers such as atrial natriuretic peptide (ANP), skeletal muscle actin (SKMactin) and cardiac fibrosis markers such as procollagen I and III, thrombospondin 1, and osteopontin were measured ( $n = 5-6$  per group). All genes were normalized to 18S level in individual samples that were measured in duplicates. In addition, PPAR $\gamma$ 1, adiponectin, and reduced nicotinamide adenine dinucleotide phosphate (NADPH) oxidase subunits (Nox2, Nox4, p22phox, p67phox) mRNA level were also quantified. Real-time polymerase chain reaction (PCR) was performed with SYBR Green technology using Prism 7900 HT system (Applied Biosystems, Warrington, UK). Primer sequences are listed in Table 1.

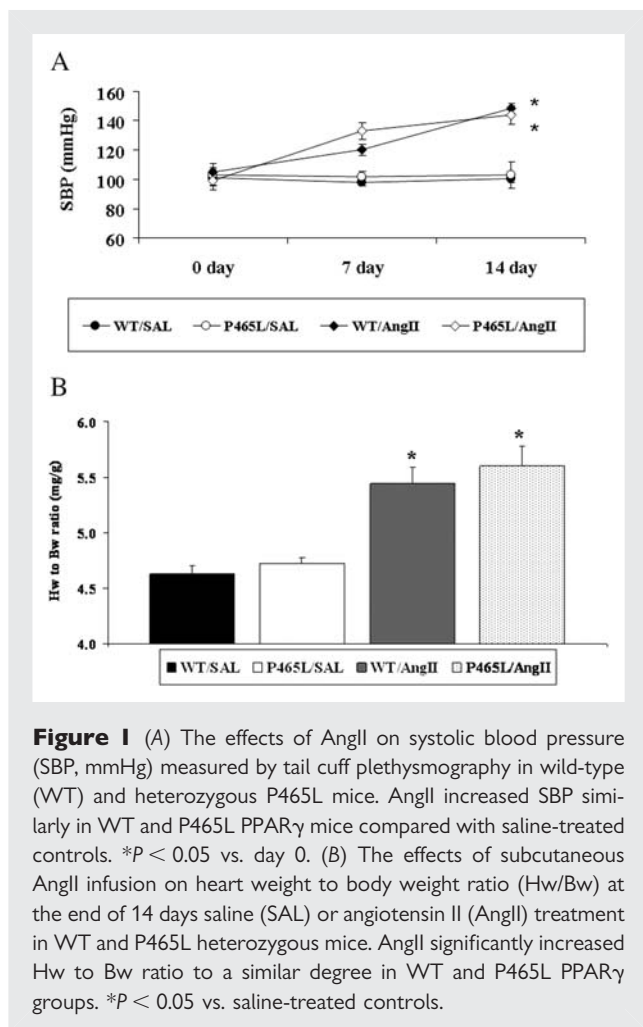
### Allele-specific reverse transcriptase-polymerase chain reaction

Forward primers: WT: 5'-gacagacatgagccttcaccc-3' detects the WT allele, whereas P465L: 5'-cagacatgagccttcacct-3' detects the mutated allele. Common reverse primer: 5'-gggtgggacttctccta-3'. Polymerase chain reaction was performed using the Power SYBR Green PCR Mastermix (Applied Biosystems) with and 100 nM primers. Cycling: 2 min at 50°C, 10 min at 95°C, then 40 cycles of 15 s at 95°C and 1 min at 66°C. These conditions were set up in order to minimize the cross amplification of alleles. To discard contaminants and RNA,

control was used we use as template for the quantitative real-time PCR under the same conditions used in the validation experiments. For mathematical analysis, the crossing points ( $C_t$ ) values were used for each transcript. The  $C_t$  is defined as the point at which fluorescence of the transcript rises significantly above the background fluorescence. The 'fit point method' was performed in the ABI7900HT platform, at which  $C_t$  was measured at a constant fluorescence level. Differences in expression between groups were assessed by Pair Wise Fixed Reallocation Randomization Test using the Relative Expression Software Tool.<sup>16</sup> Data were corrected using the geometrical average of four different housekeeping genes. Level of probability was set at  $P < 0.05$ .

### Serum biochemical parameters

Serum glucose (G), free fatty acid (FFA), cholesterol, triglyceride (TG), insulin, leptin, and adiponectin levels were determined<sup>14</sup> by commercially available tests from fed animals at the end of the 14 days treatment with AngII or saline in WT and P465L heterozygous mice. There were no significant changes in G, TG, FFA, cholesterol, insulin, and leptin levels among groups. Liver was not steatotic in any of the groups at the end of treatment. Dual-energy x-ray absorptiometry<sup>17</sup> (Lunar Corp., GE Healthcare, MD, USA) analysis confirmed that total fat percentage and body weight did not change significantly among groups.



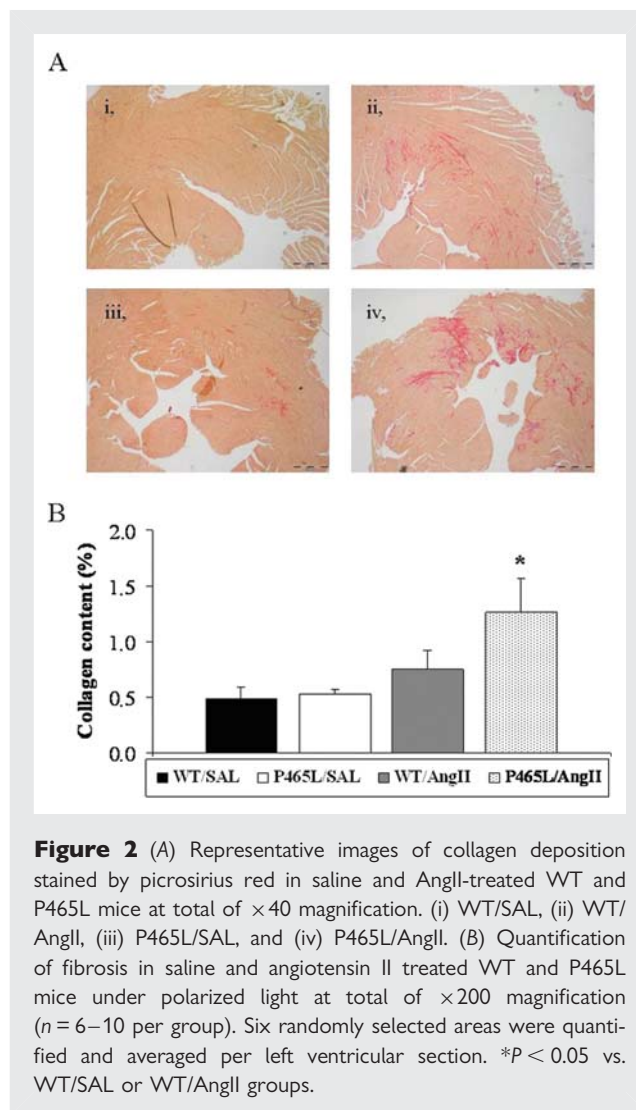
### Statistical analysis

Data are expressed as mean  $\pm$  SEM. One-way ANOVA was used to compare data among groups with Bonferroni *post hoc* test using Graphpad Prism software. Level of significance is indicated in Figures 1–5 and Table 2.

## Results

### Angiotensin II administration increases systolic blood pressure and cardiac hypertrophy to a similar extent in wild-type and P465L peroxisomal proliferators activated receptor gamma mice

We investigated the effect of chronic AngII administration on systolic blood pressure and development of cardiac hypertrophy in WT and PPAR $\gamma$  defective mice. Baseline systolic blood pressure was not significantly different between the WT and P465L heterozygous mice ( $100.9 \pm 5.8$  vs.  $103.2 \pm 7.3$  mmHg, respectively). Two weeks administration of AngII increased systolic blood pressure to a similar extent in WT and PPAR $\gamma$  defective mice. Changes in



blood pressure after 7 and 14 days of AngII treatment are shown in Figure 1. No differences were observed in basal heart weight to body weight ratio between WT/SAL mice ( $4.63 \pm 0.08$ ) and P465L/SAL mice ( $4.72 \pm 0.06$ ). As expected, AngII treatment significantly increased Hw/Bw ratio, but to a similar extent in both genotypes ( $5.44 \pm 0.15$  vs.  $5.62 \pm 0.18$ , respectively, Figure 1B).

### Increased cardiac fibrosis in angiotensin II treated P465L mice compared with wild-type mice

Despite having similar increases in blood pressure and heart hypertrophy, the PPAR $\gamma$  P465L mice developed increased fibrosis in response to AngII compared with WT littermates. Representative images (total of  $\times 40$  magnification) acquired from paraffin-embedded sections are illustrated in Figure 2A. Picrosirius red staining shows that interstitial collagen staining was minimal in saline-treated WT (i) and P465L (iii) mice, whereas chronic administration of AngII induced a cardiac fibrotic response that was more severe in P465L (iv) mice. Quantification under polarized light (total of  $\times 200$  magnifications) confirmed a similar

**Table 2** Echocardiographic parameters at day 7 and at day 14 during saline or angiotensin II treatment in wild-type and heterozygous P465L mice

	WT/SAL	P465L/SAL	WT/AngII	P465L/AngII
<b>Day 7</b>				
IVSD (mm)	0.83 $\pm$ 0.05	0.77 $\pm$ 0.03	1.02 $\pm$ 0.07*	0.98 $\pm$ 0.06*
LVESD (mm)	3.01 $\pm$ 0.07	3.22 $\pm$ 0.10	2.98 $\pm$ 0.07	3.04 $\pm$ 0.18
LVEDD (mm)	4.37 $\pm$ 0.04	4.48 $\pm$ 0.13	4.22 $\pm$ 0.10	4.31 $\pm$ 0.10
FS	31.0 $\pm$ 2.2	28.0 $\pm$ 3.2	29.3 $\pm$ 1.3	29.6 $\pm$ 3.0
HR (beats min <sup>-1</sup> )	413 $\pm$ 11	451 $\pm$ 52	480 $\pm$ 16	486 $\pm$ 20
<b>Day 14</b>				
IVSD (mm)	0.79 $\pm$ 0.01	0.82 $\pm$ 0.02	1.02 $\pm$ 0.07*	1.04 $\pm$ 0.06*
LVESD (mm)	3.37 $\pm$ 0.14	3.17 $\pm$ 0.4	3.00 $\pm$ 0.17	3.03 $\pm$ 0.19
LVEDD (mm)	4.59 $\pm$ 0.9	4.56 $\pm$ 0.12	4.25 $\pm$ 0.9	4.32 $\pm$ 0.12
FS	26.7 $\pm$ 1.7	30.3 $\pm$ 2.6	29.6 $\pm$ 2.9	30.2 $\pm$ 2.8
HR (beats min <sup>-1</sup> )	447 $\pm$ 16	477 $\pm$ 54	491 $\pm$ 29	509 $\pm$ 22

IVSD, interventricular septal thickness; LVESD, left ventricular end-systolic dimension; LVEDD, left ventricular end-diastolic dimension; FS, fractional shortening; HR, heart rate. \* $P < 0.05$  vs. WT/Sal or P465L/Sal, respectively.

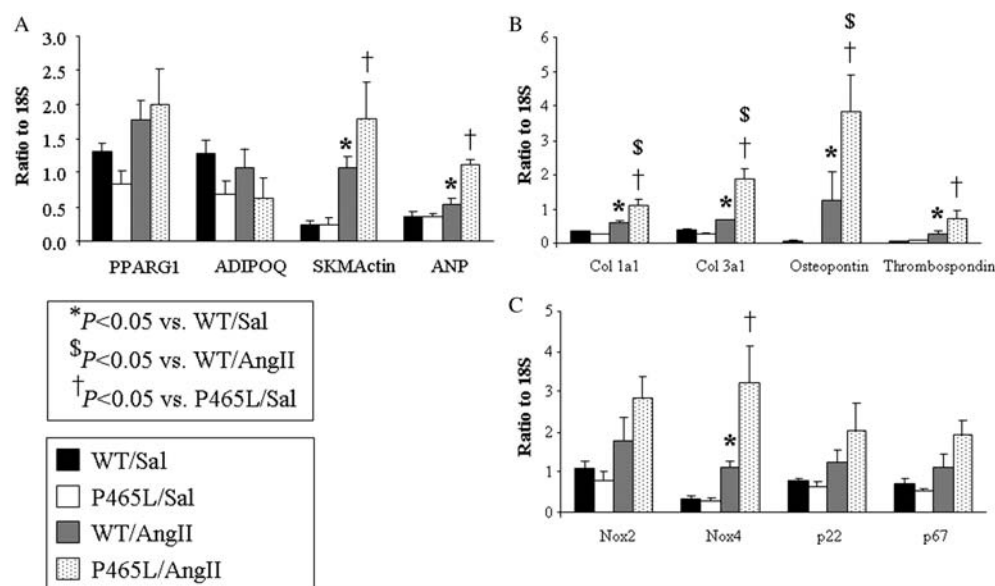


**Figure 3** Reverse transcriptase–polymerase chain reaction (RT–PCR) analysis of hypertrophy, fibrosis marker genes, and NADPH oxidase subunit genes in saline and angiotensin II treated WT and P465L mice. Expression of hypertrophy and fibrosis marker genes increased during AngII treatment; this increased expression level was higher in heterozygous P465L mice. PPAR $\gamma$ 1 and adiponectin (AdipoQ, PPAR $\gamma$  target gene) were not changed significantly among groups. \* $P < 0.05$  vs. WT/SAL; † $P < 0.05$  vs. P465L/SAL; § $P < 0.05$  vs. WT/AngII.

degree of basal fibrosis in saline-treated WT and P465L mice ( $0.48 \pm 0.1$  vs.  $0.53 \pm 0.04\%$ , respectively, Figure 2B). More importantly, AngII treatment increased fibrosis in WT mice ( $0.75 \pm 0.17\%$ , Figure 2B) by  $\sim 55\%$  compared with saline-treated WT mice, whereas heterozygous P465L treated with AngII showed a more severe 140% increase in interstitial fibrosis ( $1.27 \pm 0.3\%$ ,  $P < 0.05$  vs. WT, Figure 2B).

### Normal functional echocardiographic parameters in angiotensin II treated wild-type and P465L mice

Under the experimental conditions investigated, no differences in heart rate (Table 2) or functional parameters were found in P465L heterozygous mice and in WT littermates after 14 days

AngII treatment. As expected, AngII treatment increased inter-ventricular septal thickness by day 7 in both the WT/AngII and P465L/AngII groups to a similar extent and by day 14 no further increase in hypertrophy was detected (Table 2). Of note, both the left ventricular end-systolic and end-diastolic parameters, as well as fractional shortening were similar in WT and P465L heterozygous mice after 14 days of AngII treatment (Table 2).

### The effect of chronic angiotensin II treatment on hypertrophy and fibrosis marker genes and NADPH oxidase subunit genes

We investigated whether ANP and SKMactin, molecular markers of cardiac hypertrophy, were upregulated in our experimental model. No significant differences in basal gene expression between WT/SAL and P465L/SAL groups were observed (Figure 3A), whereas AngII-treated PPAR $\gamma$  P465L mice showed increased expression of ANP and SKMactin compared with their WT littermates (Figure 3A).

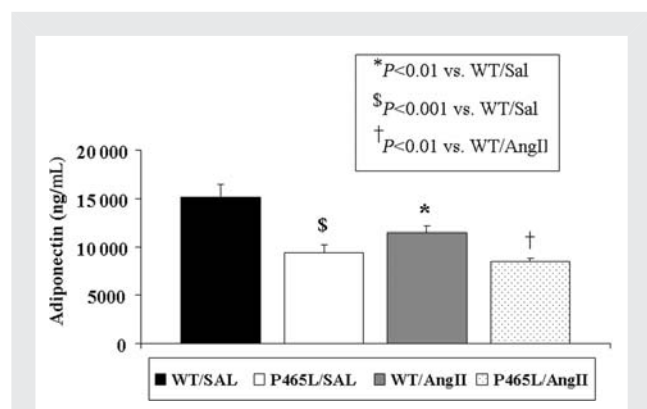


**Figure 4** Serum level of adiponectin in saline and AngII-treated WT and P465L heterozygous mice at the end of 14 days treatment. Level of significance is indicated as §P < 0.001 vs. WT/SAL; \*P < 0.01 vs. WT/SAL; †P < 0.01 vs. WT/AngII.

Similarly, expression of procollagen I and III, osteopontin, and thrombospondin1, genes encoding extracellular matrix proteins typically synthesized *de novo* during the early phase of fibrosis, was markedly upregulated in AngII-treated heterozygous P465L mice in comparison with AngII-treated WT littermates (Figure 3B). The increased expression of these fibrosis markers agreed with the increased fibrotic response observed histologically. Interestingly, basal expression level of these profibrotic genes did not significantly differ between saline-treated WT and heterozygous P465L mice (Figure 3B).

Recent studies indicate that the increased interstitial cardiac fibrosis induced by chronic AngII infusion involves the activation of NADPH oxidases, reactive oxygen species-generating enzymes involved in redox signalling and enhanced gene expression.<sup>8,15</sup> We therefore investigated whether alterations in NADPH oxidases may be involved in the enhanced profibrotic effects of AngII in mice with defective PPAR $\gamma$  function. Measurement of the relative expression of Nox2, Nox4, p22phox, and p67phox subunits of NADPH oxidase in all groups showed that only Nox4 was significantly increased in the AngII-treated P465L mice compared with AngII-treated WT mice, although the other subunits all showed a tendency to increase their mRNA level during AngII treatment (Figure 3C).

### Angiotensin II reduces adiponectin level in the serum in wild-type but not in P465L heterozygous mice

Our group has shown previously that P465L dominant-negative mutation in PPAR $\gamma$  reduces adiponectin expression in adipose tissue.<sup>14</sup> However, this decrease in adiponectin level did not result in insulin resistance in this mouse model.<sup>14</sup> We have found that, unlike in P465L heterozygous mice, AngII treatment in WT animals significantly reduced serum adiponectin level compared with saline-treated controls. Interestingly, this level remained significantly higher than that was found in AngII-treated P465L heterozygous mice (Figure 4).

### Detection of wild-type and mutant alleles in heart RNA samples

We attempted to detect mutant PPAR $\gamma$  allele in heterozygous mouse heart samples to confirm the presence of mutated allele.

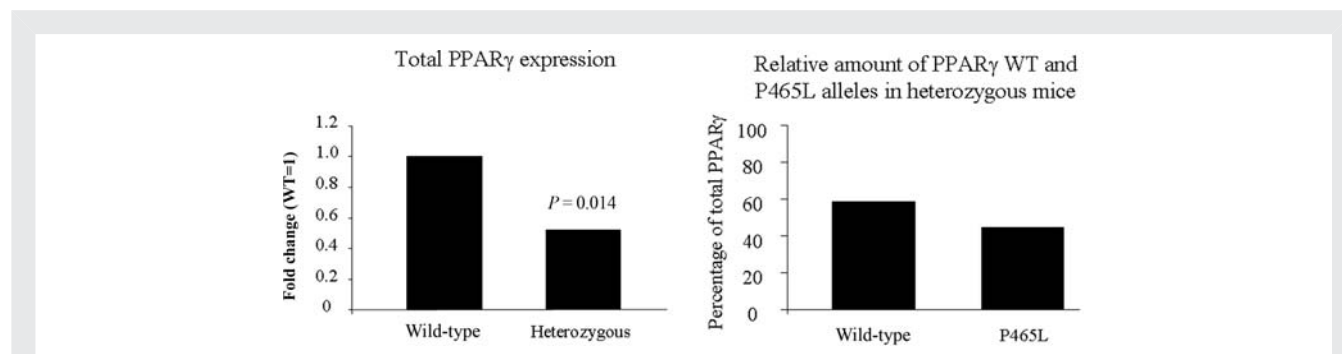


**Figure 5** Expression level of total PPAR $\gamma$  in wild-type and heterozygous mutant mice and percentage of WT and mutant PPAR $\gamma$  alleles in the heterozygous mutant mice. Level of probability was set at P < 0.05<sup>16</sup> (n = 10 per group).

This is illustrated in Figure 5. mRNA expression levels of total PPAR $\gamma$  was reduced by  $\sim$ 50% in the P465L heterozygous mice compared with WT mice. In addition to this, the WT and mutant alleles were expressed at similar levels each, one representing  $\sim$ 50% of the total PPAR $\gamma$ .

## Discussion

In this study, we show that hypertension induced by chronic AngII administration synergizes with defective PPAR $\gamma$  function *in vivo* to induce cardiac fibrosis. Using a 'humanized' knock-in mouse model recapitulating a human dominant-negative point mutation in the nuclear receptor PPAR $\gamma$ , no significant alterations were detected in basal cardiac parameters (e.g. Hw/Bw ratio) or fibrosis level. However, in the presence of AngII-induced hypertension, defective PPAR $\gamma$  activity resulted in an increased cardiac fibrosis compared with their WT littermates. This differential fibrotic response was not the result of differences in blood pressure or the degree of cardiac hypertrophy, as both WT and heterozygous P465L mice had similar increases in systolic blood pressure up to  $\sim$ 150 mmHg and their Hw to Bw ratios after AngII treatment were also similar.

Structural remodelling during sustained hypertension is a well-recognized response of the heart which typically results in both cardiomyocyte hypertrophy and interstitial fibrosis. It is driven by numerous mechanisms including mechanical stress and local and systemic neurohumoral pathways such as activation of the renin-angiotensin system. Although hypertrophy and interstitial fibrosis often co-exist, they may to a significant extent be independently regulated. The development of fibrosis involves significant rearrangement of components of the extracellular matrix, increased oxidative stress driven by NADPH oxidase,<sup>8</sup> proliferation of fibroblasts, biosynthesis of different collagen isoforms,<sup>18</sup> and the upregulation of other membrane-linked glycoproteins such as osteopontin<sup>19</sup> and thrombospondin.<sup>20</sup> It is known that severe interstitial fibrosis in response to long-term stress may be associated with diastolic dysfunction, arrhythmia, and eventually pump failure.

There is data that suggest a beneficial role of PPAR $\gamma$  in the cardiac remodelling process as indicated by pharmacological evidence that specific PPAR $\gamma$  ligands may prevent or reduce synthesis and deposition of collagen and other matrix proteins during the fibrotic response. For example, pioglitazone reduced myocardial fibrosis and collagen content during heart failure development, resulting in improved contractile function of mouse hearts.<sup>11</sup> Rosiglitazone, another PPAR $\gamma$  agonist, prevents cardiac fibrosis in mineralocorticoid induced hypertension in rats<sup>21</sup> and also, in rats subjected to aortic constriction.<sup>13</sup> Finally, ciglitazone inhibited perivascular and interstitial fibrosis in mice that underwent aortic banding, with concomitant improvement of heart function.<sup>3</sup>

Using a genetic approach, we have shown in the present study that in the presence of AngII-induced hypertension, expression of the P465L PPAR $\gamma$  human mutation is associated with increased expression of profibrotic genes such as procollagen I, III, and osteopontin. Previous data have suggested the involvement of osteopontin in myocardial fibrosis and in fact, mice lacking osteopontin are unable to develop fibrosis resulting in accelerated

myocardium dilation.<sup>22</sup> Our data indicate that osteopontin is barely expressed in the heart of WT and our PPAR $\gamma$  P465L mice, after AngII-induced hypertension osteopontin is increased up to 17-fold in WT and up to 35-fold in the P465L mice. Other examples of profibrotic genes are thrombospondin 1 and 2, both important regulators of extracellular matrix remodelling by activating TGF- $\beta$ . More specifically, there is evidence that thrombospondin 2 seems to contribute to the progression of human heart failure.<sup>20</sup> In our study, we found that heterozygous P465L mice had increased thrombospondin 1 level compared with WT mice after AngII treatment and in agreement with increased histological evidence of cardiac fibrosis we also found an increased expression collagen isoforms. Previous studies have suggested that stimulation with extrinsic PPAR $\gamma$  agonists exerts an anti-fibrotic effect, whereas the current study indicates that endogenous PPAR $\gamma$  may exert anti-fibrotic effects in the context of hypertension, which are absent in the heterozygous P465L mice. In keeping with this idea, a direct transcriptional repressing effect of PPAR $\gamma$  has been already shown for osteopontin expression through its binding to a PPAR response element sequence in the osteopontin promoter.<sup>23</sup> There is also evidence that PPAR $\gamma$  dysfunction may directly potentiate collagen synthesis through the interaction of the CIITA/RFX5 transcription factor complex on the collagen gene promoter.<sup>24</sup> Taken together, these data suggest that in our mouse model the presence of the dominant-negative PPAR $\gamma$  mutation may have impaired the repressor function of PPAR $\gamma$  in preventing cardiac fibrosis during AngII challenge, thereby allowing enhanced transcription of these particular profibrotic genes.

In contrast to the data regarding interstitial fibrosis, angiotensin II did not increase Hw to Bw ratio or Hw to tibia length (data not shown) in heterozygous P465L mice relative to WT mice. This suggests that the pro-fibrotic effects associated with this specific mutant of PPAR $\gamma$  in the presence of increased AngII levels are distinct from mechanisms driving cardiac hypertrophy at least under these experimental conditions, in contrast to previous studies.<sup>10</sup> We also found that there was no overt contractile dysfunction in the heterozygous P465L mice compared with WT mice as assessed by echocardiography, although the presence of more subtle differences remains possible and would require *in vivo* analyses and/or more prolonged treatment to exclude.

Previous data suggest that decreased adiponectin expression may be implicated in heart failure progression in humans.<sup>25</sup> Furthermore, in a similar experimental model to ours, adiponectin KO mice during AngII-induced hypertension showed substantially increased interstitial fibrosis as well as cardiac hypertrophy than their WT littermates.<sup>26</sup> In a permanent ligation induced chronic heart failure model, the lack of adiponectin significantly increased the level of compensatory hypertrophy, interstitial fibrosis, and left ventricular dysfunction.<sup>27</sup> On the contrary, in the same study, adiponectin via adenoviral delivery in WT animals protected the heart against these consequences of chronic ligation of LAD suggesting anti-fibrotic role of adiponectin.<sup>27</sup> In our mouse model, P465L dominant-negative mutation in PPAR $\gamma$  reduced adiponectin expression in the heart and adipose tissue (indicated by lower serum level) which may be contributory to the increased level of cardiac fibrosis under hypertensive conditions. We suggest that reduced adiponectin level in the absence of insulin

resistance during this initial phase of hypertension may contribute to increased cardiac fibrosis before left ventricular dysfunction occurs. However, this hypothesis needs confirmation by further studies.

Our mouse model is not insulin resistant in contrast to humans, a difference that likely arises due to discrepancy in the distribution and function of their various fat pads.<sup>28</sup> Nevertheless, both direct and indirect roles of adipose tissue in blood pressure regulation (e.g. perivascular fat) and heart function (e.g. epicardial fat) have been established in humans as well as in animal models. For example, adipokines such as leptin<sup>29</sup> and visfatin<sup>30</sup> in mice have been shown to directly regulate cardiac function under experimental conditions. In addition, insulin resistance depends on the array of adipokines secreted by various visceral and subcutaneous fat pads underlying one particular pathomechanism of the metabolic syndrome in humans.<sup>1,31,32</sup> The observed increased fibrotic cardiac (and not metabolic) phenotype in our study in heterozygous P465L mice under hypertension may be the result of altered expression of PPAR $\gamma$  target genes such as adiponectin in the heart and fat (Figures 3 and 4) but not of leptin. Similar to those humans with dominant-negative mutation in PPAR $\gamma$ ,<sup>1</sup> P465L heterozygous mice also have lower expression of adiponectin in adipose tissue as well as in the heart. Another adipose secreted adipokine, leptin which is not regulated by PPAR $\gamma$  shows no correlation with any of the phenotypes in the presence of the mutation in humans<sup>1</sup> and in our study (data not shown).

From the point of view of relevance to human disease, our data suggest that patients harbouring this mutation or similar ones<sup>31,32</sup> may be at increased risk of developing cardiac fibrosis particularly in the context of hypertension. The use of our P465L PPAR $\gamma$  mouse model to study the role of PPAR $\gamma$  in the heart has the advantage that this mouse model has a much less severe metabolic phenotype than in humans,<sup>28</sup> at least when animals are not in positive energy balance.<sup>14</sup> Thus, elucidation of the synergistic effect between defective PPAR $\gamma$  function and cardiac-specific fibrotic response in this murine model is facilitated in the absence of other complex metabolic phenotypes.

Although these PPAR $\gamma$  mutations are rare in humans,<sup>31,32</sup> these patients exist and in fact it may be possible that their prevalence may increase as increased knowledge allows targeting of specific subsets of patients such as, for example, patients with cardiac phenotypes. Our observations should emphasise that control of blood pressure in these patients may be of paramount importance to prevent cardiac-specific complications. Another less obvious implication is the relevance that these observations may have in the management of more common forms of metabolic syndrome. There is evidence from animal models and studies in humans that in parallel with the development of obesity, insulin resistance, and metabolic alterations, levels of PPAR $\gamma$  tend to decrease initiating a vicious cycle leading to metabolic failure.<sup>33</sup> This suggests that decreased PPAR $\gamma$  levels in these patients may synergise with highly prevalent hypertension to accelerate cardiac fibrosis. Thus, these considerations should fuel future translational research in humans to elucidate the relevance of the synergy between PPAR $\gamma$  agonism and hypertension in humans.

In summary, here we provide evidence using a humanized mouse model recapitulating a well-characterized human mutation that defective PPAR $\gamma$  function synergises with high blood pressure to induce cardiac fibrosis *in vivo*. This observation indicates that control of blood pressure should be prioritized in patients affected by these PPAR $\gamma$  mutations to prevent cardiac complications. We speculate that the knowledge obtained from these experiments also supports the need for strict blood pressure control in other forms of obesity and insulin resistant states where levels of PPAR $\gamma$  may be decreased in the context of the metabolic syndrome.

## Acknowledgements

Thanks to Sophie Gough for help in editing the manuscript.

## Funding

A.M.S. is supported by the British Heart Foundation (RG/03/008). A.K., C.M., M.Z., and A.V.P. were supported by BHF. A.V.P. is supported by an MRC career establishment award and MRC CORD. S.G. was supported by Diabetes UK, and M.B. by Wellcome Trust Integrative Physiology Award.

**Conflict of interest:** none declared.

## References

1. Savage DB, Tan GD, Acerini CL, Jebb SA, Agostini M, Gurnell M, Williams RL, Umpleby AM, Thomas EL, Bell JD, Dixon AK, Dunne F, Boiani R, Cinti S, Vidal-Puig A, Karpe F, Chatterjee VK, O'Rahilly S. Human metabolic syndrome resulting from dominant-negative mutations in the nuclear receptor peroxisome proliferator-activated receptor-gamma. *Diabetes* 2003;**52**:910–917.
2. Chiquette E, Ramirez G, Defronzo R. A meta-analysis comparing the effect of thiazolidinediones on cardiovascular risk factors. *Arch Intern Med* 2004;**164**:2097–2104.
3. Henderson BC, Sen U, Reynolds C, Moshal KS, Ovechkin A, Tyagi N, Kartha GK, Rodriguez WE, Tyagi SC. Reversal of systemic hypertension-associated cardiac remodeling in chronic pressure overload myocardium by ciglitazone. *Int J Biol Sci* 2007;**3**:385–392.
4. Nissen SE, Wolsky K. Effect of rosiglitazone on the risk of myocardial infarction and death from cardiovascular causes. *N Engl J Med* 2007;**24**:2457–2471.
5. Home PD, Pocock SJ, Beck-Nielsen H, Gomis R, Hanefeld M, Jones NP, Komajda M, McMurray JJ, RECORD Study Group. Rosiglitazone evaluated for cardiovascular outcomes—an interim analysis. *N Engl J Med* 2007;**357**:28–38.
6. Berk BC, Fujiwara K, Lehoux S. ECM remodeling in hypertensive heart disease. *J Clin Invest* 2007;**117**:568–575.
7. Aidietis A, Laucevicius A, Marinskis G. Hypertension and cardiac arrhythmias. *Curr Pharm Des* 2007;**13**:2545–2555.
8. Johar S, Cave AC, Narayanapanicker A, Grieve DJ, Shah AM. Aldosterone mediates angiotensin II-induced interstitial cardiac fibrosis via a Nox2-containing NADPH oxidase. *FASEB J* 2006;**20**:1546–1548.
9. Yamamoto K, Ohki R, Lee RT, Ikeda U, Shimada K. Peroxisome proliferator-activated receptor gamma activators inhibit cardiac hypertrophy in cardiac myocytes. *Circulation* 2001;**104**:1670–1675.
10. Asakawa M, Takano H, Nagai T, Uozumi H, Hasegawa H, Kubota N, Saito T, Masuda Y, Kadowaki T, Komuro I. Peroxisome proliferator-activated receptor gamma plays a critical role in inhibition of cardiac hypertrophy *in vitro* and *in vivo*. *Circulation* 2002;**105**:1240–1246.
11. Shiomi T, Tsutsui H, Hayashidani S, Suematsu N, Ikeuchi M, Wen J, Ishibashi M, Kubota T, Egashira K, Takeshita A. Pioglitazone, a peroxisome proliferator-activated receptor-gamma agonist, attenuates left ventricular remodeling and failure after experimental myocardial infarction. *Circulation* 2002;**106**:3126–3132.
12. Geng DF, Wu W, Jin DM, Wang JF, Wu YM. Effect of peroxisome proliferator-activated receptor gamma ligand. Rosiglitazone on left ventricular remodeling in rats with myocardial infarction. *Int J Cardiol* 2006;**113**:86–91.
13. Rose M, Balakumar P, Singh M. Ameliorative effect of combination of fenofibrate and rosiglitazone in pressure overload-induced cardiac hypertrophy in rats. *Pharmacology* 2007;**80**:177–184.



14. Gray SL, Dalla Nora E, Grosse J, Manieri M, Stoeger T, Medina-Gomez G, Burling K, Wattler S, Russ A, Yeo GS, Chatterjee VK, O'Rahilly S, Voshol PJ, Cinti S, Vidal-Puig A. Leptin deficiency unmasks the deleterious effects of impaired peroxisome proliferator activated receptor gamma function (P465L PPARgamma) in mice. *Diabetes* 2006;**55**:2669–2677.
15. Looi YH, Grieve DJ, Siva A, Walker SJ, Anilkumar N, Cave AC, Marber M, Monaghan MJ, Shah AM. Involvement of Nox2 NADPH oxidase in adverse cardiac remodeling after myocardial infarction. *Hypertension* 2008;**51**:319–325.
16. Pfaffl MW, Horgan GW, Dempfle L. Relative expression software tool (REST) for group-wise comparison and statistical analysis of relative expression results in real-time PCR. *Nucleic Acids Res* 2002;**30**:E36.
17. Mazess RB, Barden HS, Bisek JP, Hanson J. Dual-energy X-ray absorptiometry for total-body and regional bone-mineral and soft-tissue composition. *Am J Clin Nutr* 1990;**51**:1106–1112.
18. Larkin JE, Frank BC, Gaspard RM, Duka I, Gavras H, Quackenbush J. Cardiac transcriptional response to acute and chronic angiotensin II treatments. *Physiol Genomics* 2004;**18**:152–166.
19. Ashizawa N, Graf K, Do YS, Nunohiro T, Giachelli CM, Meehan WP, Tuan TL, Hsueh WA. Osteopontin is produced by rat cardiac fibroblasts and mediates AT(II)-induced DNA synthesis and collagen gel contraction. *J Clin Invest* 1996;**98**:2218–2227.
20. Schroen B, Heymans S, Sharma U, Blankesteyn WM, Pokharel S, Cleutjens JP, Porter JG, Evelo CT, Duisters R, van Leeuwen RE, Janssen BJ, Debets JJ, Smits JF, Daemen MJ, Crijns HJ, Bornstein P, Pinto YM. Thrombospondin-2 is essential for myocardial matrix integrity: increased expression identifies failure-prone cardiac hypertrophy. *Circ Res* 2004;**95**:515–522.
21. Iglarz M, Touyz RM, Viel EC, Paradis P, Amiri F, Diep QN, Schiffrin EL. Peroxisome proliferator-activated receptor-alpha and receptor-gamma activators prevent cardiac fibrosis in mineralocorticoid-dependent hypertension. *Hypertension* 2003;**42**:737–743.
22. Matsui Y, Jia N, Okamoto H, Kon S, Onozuka H, Akino M, Liu L, Morimoto J, Rittling SR, Denhardt D, Kitabatake A, Ueda T. Role of osteopontin in cardiac fibrosis and remodeling in angiotensin II-induced cardiac hypertrophy. *Hypertension* 2004;**43**:1195–1101.
23. Oyama Y, Akuzawa N, Nagai R, Kurabayashi M. PPARgamma ligand inhibits osteopontin gene expression through interference with binding of nuclear factors to A/T-rich sequence in THP-1 cells. *Circ Res* 2002;**90**:348–355.
24. Xu Y, Farmer SR, Smith BD. Peroxisome proliferator-activated receptor gamma interacts with CIITA x RFX5 complex to repress type I collagen gene expression. *J Biol Chem* 2007;**282**:26046–26056.
25. Skurk C, Wittchen F, Suckau L, Witt H, Noutsias M, Fechner H, Schultheiss HP, Poller W. Description of a local cardiac adiponectin system and its deregulation in dilated cardiomyopathy. *Eur Heart J* 2008;**29**:1168–1180.
26. Fujita K, Maeda N, Sonoda M, Ohashi K, Hibuse T, Nishizawa H, Nishida M, Hiuge A, Kurata A, Kihara S, Shimomura I, Funahashi T. Adiponectin protects against angiotensin II-induced cardiac fibrosis through activation of PPAR-alpha. *Arterioscler Thromb Vasc Biol* 2008;**28**:863–870.
27. Shibata R, Izumiya Y, Sato K, Papanicolaou K, Kihara S, Colucci WS, Sam F, Ouchi N, Walsh K. Adiponectin protects against the development of systolic dysfunction following myocardial infarction. *J Mol Cell Cardiol* 2007;**42**:1065–1074.
28. Tsai YS, Kim HJ, Takahashi N, Kim HS, Hagaman JR, Kim JK, Maeda N. Hypertension and abnormal fat distribution but not insulin resistance in mice with P465L PPARgamma. *J Clin Invest* 2004;**114**:240–249.
29. Smith CC, Mocanu MM, Davidson SM, Wynne AM, Simpkin JC, Yellon DM. Leptin, the obesity-associated hormone, exhibits direct cardioprotective effects. *Br J Pharmacol* 2006;**149**:5–13.
30. Lim SY, Davidson SM, Paramanathan AJ, Smith CC, Yellon DM, Hausenloy DJ. The novel adipocytokine visfatin exerts direct cardioprotective effects. *J Cell Mol Med* 2008;**12**:1395–1403.
31. Agostini M, Schoenmakers E, Mitchell C, Szatmari I, Savage D, Smith A, Rajanayagam O, Semple R, Luan J, Bath L, Zalin A, Labib M, Kumar S, Simpson H, Blom D, Marais D, Schwabe J, Barroso I, Trembath R, Wareham N, Nagy L, Gurnell M, O'Rahilly S, Chatterjee K. Non-DNA binding, dominant-negative, human PPARgamma mutations cause lipodystrophic insulin resistance. *Cell Metab* 2006;**4**:303–311.
32. Barroso I, Gurnell M, Crowley VE, Agostini M, Schwabe JW, Soos MA, Maslen GL, Williams TD, Lewis H, Schafer AJ, Chatterjee VK, O'Rahilly S. Dominant negative mutations in human PPARgamma associated with severe insulin resistance, diabetes mellitus and hypertension. *Nature* 1999;**402**:880–883.
33. Vidal-Puig A, Jimenez-Liñan M, Lowell BB, Hamann A, Hu E, Spiegelman B, Flier JS, Moller DE. Regulation of PPAR gamma gene expression by nutrition and obesity in rodents. *J Clin Invest* 1996;**97**:2553–2561.